Article

Addressing the Needle in a Haystack Problem in Time Behavioural Study of 3rd Order Gene Combinations in WNT3A Stimulated HEK 293 Cells

Shriprakash Sinha [*]

Article

Addressing the Needle in a Haystack Problem in Time Behavioural Study of 3rd Order Gene Combinations in WNT3A Stimulated HEK 293 Cells [†]

Shriprakash Sinha (ID)

Independent Researcher, 104-Madhurisha Heights Phase 1, Risali, Bhilai-490006, India; sinha.shriprakash@yandex.com
Aspects of unpublished work were presented in a poster session at the first Wnt Gordon Research Conference, from 6-11 August 2017, held in Stowe, VT 05672, USA
[†] Behavioural study of 3-odr gene comb. in WNT3A stimulated cells.

Abstract: Gujral and MacBeath [1] provides a quantitative, and dynamic study of WNT3A-mediated stimulation of HEK 293 cells, where they record time based expression profiles of several response genes which correlated significantly with proliferation and migration. By monitoring the dynamics of gene expression using self-organizing maps, they identified clusters of genes that exhibit similar expression dynamics and uncovered previously unrecognized positive and negative feedback loops. However, their study depicts/uses singular measurements of individual gene expression at different time snapshots/points to infer the system wide analysis of the WNT pathway. At any particular time point, it is often the case that genes are working synergistically in combinations, even though their expression measurements are singular in nature. Sinha [2] recently demonstrated the use of machine learning based search engine to rank/reveal gene combinations at 2nd order for the time series data by Gujral and MacBeath [1] and showed how it is possible to locate combinations of priority that might be working synergistically. However, the problem explodes combinatorially with even a small set of 71 recorded genes in the above study, when one steps to explore 3rd order combinations. With the total number of C_3^{71} (= 57155) combinations, it becomes nearly impossible for any biologist to study the system wide dynamics of any pathway. Here, I ● enumerate and rank all C_3^{71} combinations using four different sensitivity methods; ● show the conserved rankings for PORCN-WNT-X combinations, which point to existence of biological synergy of some of these combinations across the different sensitivity methods; and ● study the behaviour of some of the combinations related to WNT3A response genes that are ranked by the search engine in time. This study demonstrates how biologists can use the machine learning based search engine to address the needle in a haystack problem of discovering meaningful combinations of higher order in a vast search forest, which on further wet lab test might assist in intervening the pathway at a combinatorial level, in time.

Keywords: sensitivity analysis; support vector ranking; Hilbert Schmidt Independence Criterion indices (HSIC) and Sobol indicies; WNT3A

---

1. Integration, Innovation and Insight

At any particular time point, it is often the case that genes are working synergistically in combinations, even though their expression measurements are singular in nature. The problem explodes combinatorially with even a small set of recorded genes, when one steps to explore higher (here 3rd) order combinations. With the huge total number of combinations, it becomes nearly impossible for any biologist to study the system wide dynamics of any pathway as well as locate combinations of genuine interest. This study demonstrates how biologists can use a machine learning based search engine to address the needle in a haystack problem of discovering meaningful combinations of higher order in a vast search forest, while cutting down the time required to search the same. Further wet lab test might assist in intervening the pathway at a combinatorial level, in time.

2. Significance

Sinha [2] recently demonstrated the use of machine learning based search engine to rank/reveal gene combinations at 2nd order for the time series data by Gujral and MacBeath [1] and showed how it is possible to locate combinations of priority that might be working synergistically, using sensitivity methods and powerful support vector ranking algorithm. However, the problem explodes combinatorially with even a small set of 71 recorded genes in the study by Gujral and MacBeath [1], when one steps to explore 3rd order combinations. With the total number of $^{71}C_3$ (= 57155) combinations, it becomes nearly impossible for any biologist to study the system wide dynamics of any pathway. Also, the amount of time usually needed to search for and test a combination is far more than the search down by the machine learning based search engine. Here, I extend the research work by Sinha [2] to conduct a behavioral study of 3rd order gene combinations using individual gene expressions measured in time, in WNT3A stimulated HEK 293 cells. [1]

3. Introduction

The details of the machine learning based search engine has been recently published in Sinha [2] and deployed to explore the 2nd order combinations of genes in the data set provided by Gujral and MacBeath [1]. Nevertheless, here, I point to the fundamentals of the published work for completeness.

3.1. A Combinatorial Problem

Sensitivity analysis plays a major role in computing the strength of the influence of involved factors in any phenomena under investigation. When applied to expression profiles of various intra/extracellular factors that form an integral part of a signaling pathway, the variance and density based analysis yields a range of sensitivity indices for individual as well as various combinations of factors. These combinations denote the higher order interactions among the involved factors. Computation of higher order interactions is often time consuming but it gives a chance to explore the various combinations that might be of interest in the working mechanism of the pathway. For example, in a range of fourth order combinations among the various factors of the Wnt pathway, it would be easy to assess the influence of the destruction complex formed by APC, AXIN, CSKI and GSK3 interaction. But the effect of these combinations vary over time as measurements of fold changes and deviations in fold changes vary. So it is imperative to know how an interaction or a combination of the involved factors behave in time and Sinha [2] develops a procedure to track the behaviour by exploiting the influences of these involved factors.

3.2. A Possible Solution

In this work, after estimating the individual effects of factors for a higher order combination, the individual indices are considered as discriminative features. A combination, then, is a feature set in higher order (≥ 2 ,i.e multivariate). With an excessively large number of factors involved in the pathway, it is difficult to search for important combinations in a wide search space over different orders. Exploiting the analogy with the issues of prioritizing webpages using ranking algorithms, for a particular order, a full set of combinations of interactions can then be prioritized based on these features using a powerful ranking algorithm via support vectors Joachims [3]. Recording the changing rankings of the combinations over time reveals how higher order interactions behave within the pathway and when an intervention might be necessary to influence the interaction within the pathway.

3.3. Wnt Signaling and Secretion

Sharma [4]'s accidental discovery of the Wingless played a pioneering role in the emergence of a widely expanding research field of the Wnt signaling pathway. A majority of the work has focused on issues related to ● the discovery of genetic and epigenetic factors affecting the pathway Thorstensen

---

[1] Aspects of unpublished work presented as poster in the Berkeley Cell Symposyia : Technology, Biology & Data Science, 2016, Berkeley, USA

et al. [5] & Baron and Kneissel [6], ● implications of mutations in the pathway and its dominant role on cancer and other diseases Clevers [7], ● investigation into the pathway's contribution towards embryo development Sokol [8], homeostasis Pinto et al. [9] & Zhong et al. [10] and apoptosis Pećina-Šlaus [11] and ● safety and feasibility of drug design for the Wnt pathway Kahn [12], Garber [13], Voronkov and Krauss [14], Blagodatski et al. [15] & Curtin and Lorenzi [16].

The Wnt phenomena can be roughly segregated into signaling and secretion part. The Wnt signaling pathway works when the WNT ligand gets attached to the Frizzled(FZD)/LRP coreceptor complex. FZD may interact with the Dishevelled (DVL) causing phosphorylation. It is also thought that Wnts cause phosphorylation of the LRP via casein kinase 1 (CK1) and kinase GSK3. These developments further lead to attraction of Axin which causes inhibition of the formation of the degradation complex. The degradation complex constitutes of AXIN, the β-catenin transportation complex APC, CK1 and GSK3. When the pathway is active the dissolution of the degradation complex leads to stabilization in the concentration of β-catenin in the cytoplasm. As β-catenin enters into the nucleus it displaces the GROUCHO and binds with transcription cell factor TCF thus instigating transcription of Wnt target genes. GROUCHO acts as lock on TCF and prevents the transcription of target genes which may induce cancer. In cases when the Wnt ligands are not captured by the coreceptor at the cell membrane, AXIN helps in formation of the degradation complex. The degradation complex phosphorylates β-catenin which is then recognised by F BOX/WD repeat protein β-TRCP. β-TRCP is a component of ubiquitin ligase complex that helps in ubiquitination of β-catenin thus marking it for degradation via the proteasome.

Contrary to the signaling phenomena, the secretion phenomena is about the release and transportation of the WNT protein/ligand in and out of the cell, respectively. Briefly, the WNT proteins that are synthesized with the endoplasmic reticulum (ER), are known to be palmitoyleated via the Porcupine (PORCN) to form the WNT ligand, which is then ready for transportation. It is believed that these ligands are then transported via the EVI/WNTLESS transmembrane complex out of the cell Bänziger et al. [17] & Bartscherer et al. [18]. The EVI/WNTLESS themselves are known to reside in the Golgi bodies and interaction with the WNT ligands for the later's glycosylation Kurayoshi et al. [19] & Gao and Hannoush [20]. Once outside the cell, the WNTs then interact with the cell receptors, as explained in the foregoing paragraph, to induce the Wnt signaling. Of importance is the fact that the EVI/WNTLESS also need a transporter in the from of a complex termed as Retromer.

4. Methods

Please refer to sections of Sinha [2] for methods, design of study and analysis of data for 2nd order combinations. The same method and design of study is used to generate results for 3rd order combinations presented in this study.

5. Time Series Data

Gujral and MacBeath [1] present a set of 71 WNT-related gene expression values for 6 different times points over a range of 24-hour period using qPCR. The changes represent the fold-change in the expression levels of genes in 200 ng/mL WNT3A-stimulated HEK 293 cells in time relative to their levels in unstimulated, serum-starved cells at 0-hour. Gujral and MacBeath [1] state that qPCR data are the means of three biological replicates. Only genes whose mean transcript levels changed by more than two-fold at one or more time points during the 24-hour time course were considered significant. Positive (negative) numbers represent up (down) -regulation. We have already covered the issues related to these data sets in detail in Sinha [21]. Readers are requested to go through them in the pointed reference. The tools of study which are used here have been published in another foundational work in Sinha [21].

6. Design of Experiment
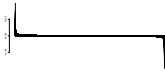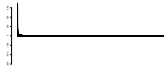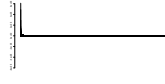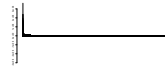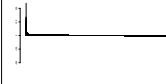
6.1. Pipeline for Time Series Data

For the case of time series data, interactions among the contributing factors are studied by comparing triplets of fold-changes at single time points. The prodecure begins with the generation of distribution around measurements at single time points with added noise is done to estimate the indices. A distribution is generated for the fold changes at single time points. Then for every gene, there is a vector of values representing fold changes as well as deviations in fold changes for different time points and durations between time points, respectively. Next a listing of all C_k^n combinations for k number of genes from a total of n genes is generated. k is ≥ 2 and $\leq (n-1)$. Each of the combination of order k represents a unique set of interaction between the involved genetic factors. After this, the datasets are combined in a specifed format which go as input as per the requirement of a particular sensitivity analysis method. Thus for each pth combination in C_k^n combinations, the dataset is prepared in the required format from the distributions for two separate cases which have been discussed above. (See .R code in mainScript-1-1.R). After the data has been transformed, vectorized programming is employed for density based sensitivity analysis and looping is employed for variance based sensitivity analysis to compute the required sensitivity indices for each of the p combinations. This procedure is done for different kinds of sensitivity analysis methods.

After the above sensitivity indices have been stored for each of the pth combination, the next step in the design of experiment is conducted. Since there is only one recording of sensitivity index per combination, each combination forms a training example which is alloted a training index and the sensitivity indices of the individual genetic factors form the training example. Thus there are C_k^n training examples for k^{th} order interaction. Using this training set SVM_{learn}^{Rank} Joachims [3] is used to generate a model on default value C value of 20. In the current experiment on toy model C value has not been tunned. The training set helps in the generation of the model as the different gene combinations are numbered in order which are used as rank indices. The model is then used to generate score on the observations in the testing set using the $SVM_{classify}^{Rank}$ Joachims [3]. Note that due to availability of only one example per combination, after the model has been built, the same training data is used as test data to generates the scores. This procedure is executed for each and every sensitivity analysis method. This is followed by sorting of these scores along with the rank indices (i.e the training indices) already assigned to the gene combinations. The end result is a sorted order of the gene combinations based on the ranking score learned by the SVM^{Rank} algorithm. Finally, this entire procedure is computed for sensitivity indices generated for each and every fold change at time point and deviations in fold change at different durations. Observing the changing rank of a particular combination at different times and different time periods will reveal how a combination is behaving.

Note that the following is the order in which the files should be executed in R, in order, for obtaining the desired results (Note that the code will not be explained here) - • use source("mainScript-1-1.R") with arguments for Dynamic data • source("SVMRank-Results-D.R"), to rank the interactions (again this needs to be done separately for different kinds of SA methods), • use source("Combine-Time-files.R"), if computing indices separately via previous file, • source("Sort-n-Plot-D.R") to sort the interactions. Note that the sorting is chages the interaction ranking in time. Thus • use source("Interaction-Priority-Intime.R") to find the prioritized ranking of each and every interaction over the different time points and finally • use source("Print-Ranking-AND-Interaction-Rank.R") to print individual ranking of the required input factor with other interaction factors. Table 1 shows the ranking scores in discending order for 3rd order combinations using four different sensitivity methods (i.e rows) and at five different time points (i.e columns).

Table 1. Rows - Sensitivity methods; Columns - Time points; A graph shows the ranking scores of combinations being arranged in descending order from left to right.

Sensitivity method	Time point				
	t = 1 hr	t = 3 hr	t = 6 hr	t = 12 hr	t = 24 hr
HSIC - Linear					
HSIC - RBF					
SOBOL - 2002					
SOBOL - martinez					

7. Results & Discussion

7.1. Time Series Data by Gujral and MacBeath [1]

NOTE - Ranking was assigned on scores that were sorted in DECREASING values. So, 1 was assigned to highest score and vice versa.

Results for the 3rd order interactions are presented here. The results first discuss the behaviour of interactions across the snapshots of time using the computed sensitivities on fold change measurements per time snapshot. The analysis was done using 4 different sensitivity indices. Out of the C_3^{71} combinations, I consider/present only those combinations that show a ranking within first 10,000 out of 57,155. This choice is liberal and biologists/oncologists can have a more stricter choice as per need. Two observations are made, • the ranking of a particular combination is conserved (i.e within the 10,000 range) in a particular time point or in the early phase or late phase of WNT3A stimulation, across the majority of the four sensitivity methods, which is a strict criteria of assessment or • the ranking of a particular combination is conserved across time points/phase (i.e they are within the 10,000 range) and the majority of the four sensitivity methods, which is relaxed criteria of assessment. Applying this filter helps reveal important combinations of interest that might be working synergistically at a higher order level in the cell.

Regarding technical points of implementation, the rankings were generated without scaling/normalizing the time series data provided by Gujral and MacBeath [1]. For estimating the sensitivity indices, a small gaussian distribution using the function **rnorm** that generates a vector of normally distributed random variables given a vector length n (here 9, the 10th one is the mean/recorded gene regulation itself), a population mean μ and population standard deviation σ. The syntax for using rnorm is as follows: **rnorm(n, mean, sd)**. Further, I use the **jitter** funtion to add a little bit of noise to the data. This helps to see if the generated rankings are robust or not.

7.2. Enumeration and Ranking of $C_3^{71} = 57155$ Combinations from Gujral and MacBeath [1]

In the supplementary section, I present four files, each containing the rankings of 3rd order combinations, that wary in time (shown for 5 time points). Each file represents the rankings computed using a particular sensitivity method. A particular row represents a particular rank given by a number. Following this, are combinations taking up that particular rank at different time points. The methods used are Hilbert Schmidt Independence Criterion indices (HSIC) indices (with rbf and linear kernel in Da Veiga [22]) and Sobol indicies (with 2002 implementation in Saltelli [23] and martinez implementation in Martinez [24] and Baudin et al. [25]). Of importance to note is that using these files, one can see a which priority/ranking one wants to investigate and see what combinations are taking

up that priority in time. Changing combinations for a particular rank indicate that at a particular point in time, a particular combination might be predominant among others.

7.3. Conserved Machine Learning Rankings for Tested PORCN-WNT-X Combinations

The Drosophila segment polarity gene product Porcupine (Porc) was first identified as being necessary for processing Wingless (Wg), a Drosophila Wnt (Wnt) family member. Tanaka et al. [26] identified Mouse (Mporc) and Xenopus (Xporc) homologs of porc and found that they encode endoplasmic reticulum (ER) proteins with multiple transmembrane domains. Further, Mporc mRNA was differentially expressed during embryogenesis and in various adult tissues, demonstrating that the alternative splicing is regulated to synthesize the specific types of Mporc. In transfected mammalian cells, they found all types of Mporc affected the processing of mouse WNT1, WNT3A, WNT4, WNT6, and WNT7B but not WNT5A. Lastly, they also found that all types of Mporc co-immunoprecipitated with various WNT proteins. Their results suggested that Mporc may function as a chaperone-like molecule for WNT.

Liu et al. [27] indicate that post-translational modification of WNTs includes lipid modification and glycosylation. The former is performed by PORCN. PORCN is a membrane-bound O-acyltransferase located in the endoplasmic reticulum and can add palmitoleate groups to WNT proteins that is necessary for WNT ligand secretion, and it is a member of the membrane-bound O-acyltransferases (MBOATs). Lipid modification is necessary for Wnt activity, and the opposite is true for glycosylation as observed by Willert et al. [28]. Liu et al. [29] developed a screen for small molecules that blocked WNT secretion and discovered LGK974, a potent and specific small-molecule PORCN inhibitor. They show that LGK974 inhibits WNT signaling, including reduction of the WNT-dependent LRP6 phosphorylation and the expression of WNT target genes, like as AXIN2. The inhibitor is effective in multiple tumor models at well-tolerated doses. Together, their findings provide a strategy and and a tool for targeting WNT-driven cancers through the inhibition of PORCN. Further down the line, Madan et al. [30] developed a novel potent, orally available PORCN inhibitor, ETC-1922159 that blocked the secretion and activity of all WNTs. ETC-1922159 is remarkably effective in treating RSPO-translocation bearing colorectal cancer (CRC) patient-derived xenografts. This is the first example of effective targeted therapy for this subset of CRC. By this demonstration they show that inhibition of WNT signaling by PORCN inhibition holds promise as differentiation therapy in genetically defined human cancers.

Based on these experimental tests and documented literature, the synergy of PORCN-WNT can be used to see if the above machine learning based engine gives appropriate ranking to 3rd order combinations of PORCN-WNT-X (X, a particular gene/protein). If the rankings are appropriate, then we can infer that the search engine indeed points to combinatorial synergies, whether tested or unexplored, at biological level. Gujral and MacBeath [1] recorded the regulations of PORCN along with WNT1, WNT2B, WNT3A, WNT4 and WNT5A.

Here, I present and demonstrate the conservation of rankings of PORCN-WNT-X combinations across different sensitivity methods. Using the linear kernel and HSIC sensitivity analysis method, Table 2 shows rankings of combinations within the first 10,000 range (with low numerical value meaning a very high priority/role) mostly during the first phase (or after t = 1 hour of WNT3A stimulation). These point to the possible role of combinations during the early phase of WNT3A stimulation. As time passes, the rankings of these combinations get lower ranks (i.e higer numerical values) pointing to their down play of role when the effect of WNT3A stimulation has subsided in the late phase. These 3rd order synergies indicate the efficacy of the machine learning based search engine in finding meaningful combinations that might be of interest to (developmental)biologists, molecular biologists and oncologists.

Table 2. Rankings of PORCN-WNT-X. SA - HSIC; Kernel - linear

RANKING @ t_i USING HSIC - LINEAR

3rd order comb.	t_1	t_3	t_6	t_{12}	t_{24}	3rd order comb.	t_1	t_3	t_6	t_{12}	t_{24}
CXXC4-PORCN-WNT4	49	6186	19448	20672	51388	PITX2-PORCN-WNT4	177	16891	32175	32123	27627
FZD6-PORCN-WNT2B	379	19259	55786	24330	16739	FZD6-PORCN-WNT4	394	39861	46523	785	6046
FOSL1-PORCN-WNT4	455	37570	20729	10105	38487	PITX2-PORCN-WNT2B	630	42884	44910	50269	15186
FZD5-PORCN-WNT4	646	40380	25866	12816	56710	FOSL1-PORCN-WNT2B	670	19667	46545	40946	19709
KREMEN1-PORCN-WNT4	693	6753	23243	1864	44869	FZD7-PORCN-WNT3A	780	35610	948	25632	12174
DKK1-PORCN-WNT2B	1222	26601	56978	25305	51044	KREMEN1-PORCN-WNT3A	1377	25809	2588	12830	26801
BCL9-PORCN-WNT2B	1394	28608	33398	47599	21197	FZD8-PORCN-WNT4	1416	27491	15836	9789	36903
NLK-PORCN-WNT4	1742	49908	50644	30880	6042	GSK3B-PORCN-WNT4	1893	29701	28162	8296	19073
FRAT1-PORCN-WNT4	1985	2835	18017	16053	23730	FZD6-PORCN-WNT2	2024	30877	41431	1558	29140
FZD5-PORCN-WNT2B	2123	44490	45300	33310	53770	FZD6-PORCN-WNT5A	2165	41983	26329	43017	27185
CCND3-PORCN-WNT5A	2270	38617	15634	39601	37699	CXXC4-PORCN-WNT3	2291	2240	24537	6255	30135
FZD6-PORCN-WNT3A	2394	56979	41510	33895	6602	CSNK1D-PORCN-WNT5A	2899	17376	34214	55252	32946
BCL9-PORCN-WNT2	2978	30124	2987	21306	45043	DKK1-PORCN-WNT3A	3027	51411	42480	14175	39772
EP300-PORCN-WNT4	3047	52212	12666	11882	56673	LRP5-PORCN-WNT5A	3051	25077	6874	53519	30711
FZD8-PORCN-WNT2	3084	38943	6461	12608	17348	CSNK1A1-PORCN-WNT4	3257	26979	26665	9094	28864
DIXDC1-PORCN-WNT2B	3266	11238	38406	37800	51881	CSNK1G1-PORCN-WNT2	3410	20366	30313	12508	34531
FOSL1-PORCN-WNT5A	3631	16428	9587	43895	35656	DAAM1-PORCN-WNT4	3680	47587	5186	9818	24761
FZD1-PORCN-WNT2	3737	14464	10387	26137	31141	EP300-PORCN-WNT2B	3826	37202	48507	42391	54306
DIXDC1-PORCN-WNT5A	3885	26867	8379	47688	52084	FOSL1-PORCN-WNT3A	3900	15019	1518	39920	12124
FZD2-PORCN-WNT3	3994	23668	24913	3556	38793	CSNK1A1-PORCN-WNT2B	4109	24272	43637	30113	14274
BCL9-PORCN-WNT3A	4125	17834	1540	51723	23039	FOSL1-PORCN-WNT2	4144	48973	6608	18938	40921
LEF1-PORCN-WNT3	4220	6502	35317	5065	1556	LRP6-PORCN-WNT2B	4288	11513	52986	43798	7888
CTNNB1-PORCN-WNT2B	4381	41494	54608	33159	44891	FZD5-PORCN-WNT3A	4393	44820	4226	33407	54333
GSK3B-PORCN-WNT2B	4525	24848	40685	28860	9721	FZD2-PORCN-WNT4	4576	26380	31174	13954	52829
FZD5-PORCN-WNT2	4674	42137	9005	17361	56340	EP300-PORCN-WNT5A	4719	30282	10559	49731	55789
FRAT1-PORCN-WNT5A	4744	35332	12577	52285	31329	FRAT1-PORCN-WNT3A	4941	28915	3063	37414	10241
KREMEN1-PORCN-WNT2	4959	36712	10209	2355	46390	CTNNBIP1-PORCN-WNT4	5017	38878	13233	4965	42568
FZD7-PORCN-WNT2	5063	48509	3534	18543	37452	FBXW2-PORCN-WNT5A	5093	9753	1927	56299	23944
CSNK1A1-PORCN-WNT5A	5243	23800	15741	37419	31250	FRZB-PORCN-WNT5A	5316	15372	16217	53391	42789
FZD2-PORCN-WNT2	5319	35217	4925	18448	50496	FZD6-PORCN-WNT3	5539	17206	33991	301	6205
DVL2-PORCN-WNT2B	5842	46277	40915	44683	55710	LEF1-PORCN-WNT4	5938	6340	32575	15016	39684
DIXDC1-PORCN-WNT2	6166	9846	4217	17714	53792	DVL1-PORCN-WNT2B	6171	16317	38040	29254	5289
FBXW11-PORCN-WNT2	6311	39888	7951	33180	19070	CTNNB1-PORCN-WNT5A	6382	34261	18812	36691	51406
DVL1-PORCN-WNT4	6631	47068	9083	4176	6383	FRAT1-PORCN-WNT3	6706	18258	19680	8889	11973
DAAM1-PORCN-WNT5A	6758	49371	3391	50318	25339	FBXW11-PORCN-WNT3	6762	31256	9446	8712	8411
FBXW2-PORCN-WNT2	6905	25689	1063	38513	34061	DVL1-PORCN-WNT2	7032	39563	1823	5185	12571
DKK1-PORCN-WNT3	7165	12201	52957	1425	47839	FSHB-PORCN-WNT4	7187	35341	51879	43751	30960
DIXDC1-PORCN-WNT3A	7226	9557	1088	34837	45504	APC-PORCN-WNT3	7285	26324	14843	5204	12325
CSNK2A1-PORCN-WNT2	7317	28374	7626	21080	31795	DVL2-PORCN-WNT5A	7381	46344	27348	46664	56984
NLK-PORCN-WNT3	7444	40963	56870	11439	3041	GSK3B-PORCN-WNT3A	7574	34492	6475	23367	8516
FRZB-PORCN-WNT3A	7687	8222	4498	44883	17262	CTNNBIP1-PORCN-WNT5A	7693	15781	8108	34940	32551
CSNK1G1-PORCN-WNT3A	7824	36551	31135	32075	7370	FZD7-PORCN-WNT3	7919	50229	13866	3977	19719
FBXW2-PORCN-WNT3A	8007	29570	331	44149	23392	CTNNBIP1-PORCN-WNT3	8175	33782	15052	3217	10272
FZD8-PORCN-WNT3	8198	42890	20340	2880	17514	DVL2-PORCN-WNT3A	8315	32904	22980	44056	50976
PORCN-SFRP1-WNT2B	8374	33217	32367	38609	43781	EP300-PORCN-WNT3	8497	44763	16497	4191	45957
PORCN-SFRP1-WNT5A	8531	30769	38133	56398	46745	CSNK1A1-PORCN-WNT3	8682	9887	21818	2357	12384
LRP5-PORCN-WNT3	8787	10685	15101	51335	9714	FOSL1-PORCN-WNT3	8888	41174	18861	4616	20787
AXIN1-PORCN-WNT4	9013	31986	17718	11205	34131	PORCN-WNT4-WNT5A	9093	21416	44185	36030	52780
FRAT1-PORCN-WNT2	9314	30043	8901	28853	31633	CTNNB1-PORCN-WNT3	9325	40433	31660	954	26533
GSK3B-PORCN-WNT2	9371	40431	15296	6282	27880	AES-PORCN-WNT5A	9395	43267	5747	17185	30918
FRZB-PORCN-WNT3	9560	6430	26600	4539	19524	CTBP1-PORCN-WNT3A	9567	4412	1206	29048	13053
MYC-PORCN-WNT2	9597	42141	37704	21380	33950	DAAM1-PORCN-WNT2	9600	49958	2043	12313	45710
CTNNBIP1-PORCN-WNT2	9847	23180	4750	9800	36378	FGF4-PORCN-WNT2B	9991	29929	44511	25174	44265

A total of 2415, 3rd order combinations involving PROCN were obtained from a full set of $C_3^{71} = 57155$ combinations. Out of these 2415 combinations, those related to PORCN-WNT synergy are selected. Further, from this selected set, using the above criteria for conserved rankings, I report/tabulate the meaningful combinations that might be working synergistically. Tables 3, 4 and 5 show the rankings for the same combinations as in Table 2, but using rbf kernel for HSIC, 2002 implementation for SOBOL and martinez implementation for SOBOL, respectively. As on tallies the rankings of across these tables for a particular combination, one finds that the role of the combination of interest is conserved. This conservation points to the existence of the biological synergy, whether the combination has been tested or unexplored/untested. At least at the 2nd order, considering the combinations of PORCN-WNT which have already been established in wet lab experiments (in above literature), the tabulated combinations with their appropriate ranks show the promise of the machine learning search engine in effectively locating the PORCN-WNT combinations. Further, the presented rankings point to combinations of PORCN-WNT-X, i.e the 3rd order combinations. So, considering all of the C_3^{71}

combinations, the machine learning search engine quickly ranks them and helps in tackling the needle in a haystack problem of finding combinations in a vast search forest, in a very short period of time. Even C_3^{71} is a big range of combinations to deal with, for any biologist/oncologist in a wet lab setting. The manhine learning search engine is a tool that will assist many biologists/oncologists cut the time of search and also zoom in for particular combination of interest.

Table 3. Rankings of PORCN-WNT-X. SA - HSIC; Kernel - rbf

RANKING @ t_i USING HSIC - RBF

3rd order comb.	t_1	t_3	t_6	t_{12}	t_{24}	3rd order comb.	t_1	t_3	t_6	t_{12}	t_{24}
CXXC4-PORCN-WNT4	12492	2278	24920	46755	55842	PITX2-PORCN-WNT4	9247	2492	36647	13332	52478
FZD6-PORCN-WNT2B	47	9685	16997	36922	48852	FZD6-PORCN-WNT4	49	30454	13795	53236	50505
FOSL1-PORCN-WNT4	1429	25705	30547	51837	52319	PITX2-PORCN-WNT2B	6802	25276	16938	13140	54357
FZD5-PORCN-WNT4	21655	38004	30699	16505	55082	FOSL1-PORCN-WNT2B	4296	5489	1279	29512	55035
KREMEN1-PORCN-WNT4	4572	591	18551	4045	46258	FZD7-PORCN-WNT3A	7046	46922	42358	23913	36667
DKK1-PORCN-WNT2B	6263	7902	41853	840	49894	KREMEN1-PORCN-WNT3A	8946	29482	33980	6745	37128
BCL9-PORCN-WNT2B	7648	28196	20793	10962	34371	FZD8-PORCN-WNT4	3177	7307	28634	31520	31714
NLK-PORCN-WNT4	33383	45823	7542	34942	49961	GSK3B-PORCN-WNT4	7755	14164	10378	27077	53726
FRAT1-PORCN-WNT4	6345	412	40450	45568	49626	FZD6-PORCN-WNT2	586	40987	4888	4733	51712
FZD5-PORCN-WNT2B	20497	40866	6253	29353	51974	FZD6-PORCN-WNT5A	88	50478	30280	17366	51000
CCND3-PORCN-WNT5A	12281	45137	3555	19433	30263	CXXC4-PORCN-WNT3	37775	8521	7319	54045	46168
FZD6-PORCN-WNT3A	75	57089	15014	7701	45470	CSNK1D-PORCN-WNT5A	17071	12074	1312	10487	50936
BCL9-PORCN-WNT2	28083	32378	4465	3529	55212	DKK1-PORCN-WNT3A	3656	53268	6994	22200	48539
EP300-PORCN-WNT4	5823	49192	43675	49247	45902	LRP5-PORCN-WNT5A	4664	27857	8039	7363	54523
FZD8-PORCN-WNT2	9002	35606	6653	15940	32619	CSNK1A1-PORCN-WNT4	22396	7881	36610	47685	56275
DIXDC1-PORCN-WNT2B	20111	15273	9550	18377	30375	CSNK1G1-PORCN-WNT2	21543	32722	24973	9534	56929
FOSL1-PORCN-WNT5A	684	10157	3538	9803	48095	DAAM1-PORCN-WNT4	35996	39470	9367	45869	39406
FZD1-PORCN-WNT2	16381	31579	18868	2713	56723	EP300-PORCN-WNT2B	15830	18382	7434	20043	39500
DIXDC1-PORCN-WNT5A	17412	29192	9192	10144	42283	FOSL1-PORCN-WNT3A	1761	8657	47396	12988	53731
FZD2-PORCN-WNT3	3861	10371	8475	41168	44534	CSNK1A1-PORCN-WNT2B	29063	5140	20656	25842	56335
BCL9-PORCN-WNT3A	14481	19317	37603	22307	42095	FOSL1-PORCN-WNT2	8304	49480	51245	9737	56572
LEF1-PORCN-WNT3	15283	16253	23588	39987	45869	LRP6-PORCN-WNT2B	9683	1526	19256	22267	47876
CTNNB1-PORCN-WNT2B	3504	38996	12248	21395	50262	FZD5-PORCN-WNT3A	12410	43484	27634	36130	51870
GSK3B-PORCN-WNT2B	8048	11294	10179	16139	54531	FZD2-PORCN-WNT4	695	6500	28617	20769	54707
FZD5-PORCN-WNT2	36093	40927	1182	2948	56700	EP300-PORCN-WNT5A	14385	21157	9773	23711	50138
FRAT1-PORCN-WNT5A	9891	40070	11853	25638	52101	FRAT1-PORCN-WNT3A	2312	22937	18240	22166	52333
KREMEN1-PORCN-WNT2	11953	40138	35447	19055	52764	CTNNBIP1-PORCN-WNT4	8250	26459	7633	44740	54344
FZD7-PORCN-WNT2	34943	49486	52615	11489	44146	FBXW2-PORCN-WNT5A	11096	281	22916	22682	46584
CSNK1A1-PORCN-WNT5A	18048	10911	1449	21232	54808	FRZB-PORCN-WNT5A	4873	5304	4481	15496	53540
FZD2-PORCN-WNT2	1870	34234	31607	23727	56721	FZD6-PORCN-WNT3	9106	30120	463	54159	46051
DVL2-PORCN-WNT2B	6933	36546	23445	39919	54053	LEF1-PORCN-WNT4	5168	560	21906	36211	39978
DIXDC1-PORCN-WNT2	23094	19050	12525	5084	37797	DVL1-PORCN-WNT2B	11320	1449	22904	39255	42653
FBXW11-PORCN-WNT2	12778	29459	19512	7578	56052	CTNNB1-PORCN-WNT5A	9172	29306	14624	17774	54309
DVL1-PORCN-WNT4	9417	29124	39214	53815	39945	FRAT1-PORCN-WNT3	31121	16135	7261	44737	43354
DAAM1-PORCN-WNT5A	12232	34746	14301	11892	33603	FBXW11-PORCN-WNT3	21925	17070	11142	36917	20820
FBXW2-PORCN-WNT2	15457	8876	5216	27560	28062	DVL1-PORCN-WNT2	17995	21939	25504	2801	52991
DKK1-PORCN-WNT3	40172	10975	8157	48246	47170	FSHB-PORCN-WNT4	15962	23579	8654	7169	56130
DIXDC1-PORCN-WNT3A	5822	6206	42682	5541	30451	APC-PORCN-WNT3	30579	10413	26221	51601	50456
CSNK2A1-PORCN-WNT2	25929	18590	35881	10625	56369	DVL2-PORCN-WNT5A	8044	40090	34866	13832	54387
NLK-PORCN-WNT3	50644	29189	2713	13343	42697	GSK3B-PORCN-WNT3A	3461	14490	6838	14639	54422
FRZB-PORCN-WNT3A	6749	34490	49148	22906	54377	CTNNBIP1-PORCN-WNT5A	7305	10873	2924	1222	53417
CSNK1G1-PORCN-WNT3A	21663	38683	3656	2044	55146	FZD7-PORCN-WNT3	53596	48671	6021	51770	28806
FBXW2-PORCN-WNT3A	6686	29263	3513	11200	19870	CTNNBIP1-PORCN-WNT3	33531	24069	10483	42349	51457
FZD8-PORCN-WNT3	35456	36452	36269	42228	28440	DVL2-PORCN-WNT3A	14794	20048	11512	8279	52754
PORCN-SFRP1-WNT2B	4723	27655	8331	26598	23511	EP300-PORCN-WNT3	50856	39748	37310	50396	40943
PORCN-SFRP1-WNT5A	8990	18239	20358	7994	16383	CSNK1A1-PORCN-WNT3	29342	2632	19879	55053	49188
LRP5-PORCN-WNT3	24747	9932	38589	30383	52298	FOSL1-PORCN-WNT3	18352	38735	1724	45267	50576
AXIN1-PORCN-WNT4	12916	16183	30565	49994	53220	PORCN-WNT4-WNT5A	46004	7077	13157	8574	11165
FRAT1-PORCN-WNT2	7732	25639	17621	15152	56257	CTNNB1-PORCN-WNT3	27473	34798	1060	55400	49686
GSK3B-PORCN-WNT3	7902	27843	40790	20077	56514	AES-PORCN-WNT5A	44241	42535	20909	4940	45583
FRZB-PORCN-WNT3	32861	8504	11671	40944	46353	CTBP1-PORCN-WNT3A	7201	6127	37568	36662	54763
MYC-PORCN-WNT2	20775	49804	1366	1434	56653	DAAM1-PORCN-WNT2	32528	49156	12339	6293	46115
CTNNBIP1-PORCN-WNT2	13877	15718	24186	3006	56598	FGF4-PORCN-WNT2B	49418	20740	4720	31683	48786

Table 4. Rankings of PORCN-WNT-X. SA - SOBOL; Implementation - 2002

Ranking @ t_i using SOBOL - 2002

3rd order comb.	t_1	t_3	t_6	t_{12}	t_{24}	3rd order comb.	t_1	t_3	t_6	t_{12}	t_{24}
CXXC4-PORCN-WNT4	9600	4879	1294	6463	37839	PITX2-PORCN-WNT4	38340	23219	45866	44679	30684
FZD6-PORCN-WNT2B	31884	54376	34870	43757	175	FZD6-PORCN-WNT4	12889	17968	25060	5439	42744
FOSL1-PORCN-WNT4	47380	31804	36756	47696	19151	PITX2-PORCN-WNT2B	9536	5794	12824	18961	17911
FZD5-PORCN-WNT4	9207	29406	23871	11381	42466	FOSL1-PORCN-WNT2B	9686	2290	2189	14059	39340
KREMEN1-PORCN-WNT4	2994	1634	5445	11732	52786	FZD7-PORCN-WNT3A	20917	23923	24750	6039	49403
DKK1-PORCN-WNT2B	41383	41457	40170	35729	7578	KREMEN1-PORCN-WNT3A	36088	42706	41171	37942	19003
BCL9-PORCN-WNT2B	619	12023	16698	20050	36808	FZD8-PORCN-WNT4	4950	13451	24888	5374	42530
NLK-PORCN-WNT4	3277	2846	7185	12509	42889	GSK3B-PORCN-WNT4	1508	45949	15059	14068	43601
FRAT1-PORCN-WNT4	26095	16695	23293	12549	25899	FZD6-PORCN-WNT2	25276	2810	22247	13377	56981
FZD5-PORCN-WNT2B	39424	1395	52348	50158	12675	FZD6-PORCN-WNT5A	44224	38925	32092	51688	14427
CCND3-PORCN-WNT5A	38273	8403	32926	50822	31855	CXXC4-PORCN-WNT3	13	8251	9046	18094	39176
FZD6-PORCN-WNT3A	56095	49583	38183	45187	10584	CSNK1D-PORCN-WNT5A	33173	15133	30807	39641	18354
BCL9-PORCN-WNT2	54695	186	56806	50335	13657	DKK1-PORCN-WNT3A	50877	8870	41126	42802	14055
EP300-PORCN-WNT4	30024	54987	52222	44421	1005	LRP5-PORCN-WNT5A	52695	9213	43304	43600	2584
FZD8-PORCN-WNT2	823	26064	22707	13185	36084	CSNK1A1-PORCN-WNT4	18363	33232	26729	4216	46046
DIXDC1-PORCN-WNT2B	3373	21084	13572	18388	49569	CSNK1G1-PORCN-WNT2	50216	4601	38088	29252	9325
FOSL1-PORCN-WNT5A	17862	53252	383	11834	29054	DAAM1-PORCN-WNT4	16426	28262	4305	18485	53571
FZD1-PORCN-WNT2	4082	13681	13674	16800	40849	EP300-PORCN-WNT2B	15324	657	8664	22349	56194
DIXDC1-PORCN-WNT5A	952	7968	6431	9090	46718	FOSL1-PORCN-WNT3A	9807	26119	20412	9520	38142
FZD2-PORCN-WNT3	12896	43979	25222	26252	20584	CSNK1A1-PORCN-WNT2B	32766	32478	29427	48576	29309
BCL9-PORCN-WNT3A	10614	7797	23824	20378	37147	FOSL1-PORCN-WNT2	32691	53282	55078	52635	15390
LEF1-PORCN-WNT3	1897	49638	17744	24203	37718	LRP6-PORCN-WNT2B	14001	48495	14927	23939	48458
CTNNB1-PORCN-WNT2B	21141	13797	10811	11267	27556	FZD5-PORCN-WNT3A	36290	43622	45186	48760	4106
GSK3B-PORCN-WNT2B	40100	22639	43535	41745	32288	FZD2-PORCN-WNT4	19439	3391	10054	16441	30372
FZD5-PORCN-WNT2	17667	55785	4806	7011	44403	EP300-PORCN-WNT5A	20382	5030	5420	2444	52850
FRAT1-PORCN-WNT5A	31003	40407	33852	44607	31401	FRAT1-PORCN-WNT3A	41935	48293	37010	46134	10038
KREMEN1-PORCN-WNT2	4395	4929	2983	21310	24768	CTNNBIP1-PORCN-WNT4	25654	40969	4949	17529	55280
FZD7-PORCN-WNT2	29459	48233	34006	44227	8832	FBXW2-PORCN-WNT5A	34712	23368	45069	53538	870
CSNK1A1-PORCN-WNT5A	38789	23969	30418	52936	11242	FRZB-PORCN-WNT5A	46306	37127	38922	49415	8250
FZD2-PORCN-WNT2	19066	11867	11958	13958	54152	FZD6-PORCN-WNT3	1060	2810	18960	7604	46623
DVL2-PORCN-WNT2B	29853	47974	32269	46097	48598	LEF1-PORCN-WNT4	1022	22940	10143	23171	24580
DIXDC1-PORCN-WNT2	49186	4194	44785	51431	14406	DVL1-PORCN-WNT2B	40525	45123	41427	54543	4682
FBXW11-PORCN-WNT2	23357	13473	24805	6018	45404	CTNNB1-PORCN-WNT5A	13708	4031	12259	7191	26151
DVL1-PORCN-WNT4	20685	17463	11589	4589	42885	FRAT1-PORCN-WNT3	15232	8958	20105	11048	47325
DAAM1-PORCN-WNT5A	40815	29141	52832	38755	3576	FBXW11-PORCN-WNT3	16713	4954	24116	4905	32441
FBXW2-PORCN-WNT2	21418	34494	12902	15427	45695	DVL1-PORCN-WNT2	16681	12031	15758	2629	52473
DKK1-PORCN-WNT3	6334	48097	16047	14394	43015	FSHB-PORCN-WNT4	45867	2754	36614	35679	21141
DIXDC1-PORCN-WNT3A	4460	39339	11468	317	55081	APC-PORCN-WNT3	16291	16865	6866	16198	2665
CSNK2A1-PORCN-WNT2	4020	41699	1257	21148	55149	DVL2-PORCN-WNT5A	30719	33390	31230	44148	37843
NLK-PORCN-WNT3	5701	24382	20672	24152	44887	GSK3B-PORCN-WNT3A	53885	36640	45918	41054	36072
FRZB-PORCN-WNT3A	41182	40550	43804	44778	35334	CTNNBIP1-PORCN-WNT5A	31467	16471	52175	39654	1859
CSNK1G1-PORCN-WNT3A	5826	7485	13924	24296	26101	FZD7-PORCN-WNT3	52083	39346	38543	56059	12372
FBXW2-PORCN-WNT3A	29440	19195	41476	51750	21814	CTNNBIP1-PORCN-WNT3	23703	12476	9340	1961	39642
FZD8-PORCN-WNT3	856	9226	16578	5870	42396	DVL2-PORCN-WNT3A	41245	49749	29482	36589	48546
PORCN-SFRP1-WNT2B	5304	40532	1039	12715	4309	EP300-PORCN-WNT3	41860	56501	48463	34741	957
PORCN-SFRP1-WNT5A	3180	7525	15911	15553	17157	CSNK1A1-PORCN-WNT3	23223	33035	27629	15910	40581
LRP5-PORCN-WNT3	6138	18536	4914	23077	47094	FOSL1-PORCN-WNT3	47540	54840	54984	43162	17864
AXIN1-PORCN-WNT4	23738	25185	14884	7905	7566	PORCN-WNT4-WNT5A	15387	7092	1712	7474	56642
FRAT1-PORCN-WNT2	19931	10329	16043	9132	55049	CTNNB1-PORCN-WNT3	35945	43282	46348	45906	29631
GSK3B-PORCN-WNT2	17073	34553	13631	15361	24594	AES-PORCN-WNT5A	39071	41331	43943	36584	10293
FRZB-PORCN-WNT3	15867	16647	13322	12391	21906	CTBP1-PORCN-WNT3A	31316	34389	34735	43964	25475
MYC-PORCN-WNT2	927	8233	3947	17550	45400	DAAM1-PORCN-WNT2	26110	40488	11965	20021	55712
CTNNBIP1-PORCN-WNT2	15297	27154	10616	7247	52470	FGF4-PORCN-WNT2B	30643	33813	53833	55121	19964

Table 5. Rankings of PORCN-WNT-X. SA - SOBOL; Implementation - martinez

RANKING @ t_i USING SOBOL - MARTINEZ

3rd order comb.	t_1	t_3	t_6	t_{12}	t_{24}	3rd order comb.	t_1	t_3	t_6	t_{12}	t_{24}
CXXC4-PORCN-WNT4	4276	14596	42774	57022	45130	PITX2-PORCN-WNT4	9395	23474	32883	37297	24846
FZD6-PORCN-WNT2B	5774	40911	34822	40189	42079	FZD6-PORCN-WNT4	199	7166	3089	14140	1367
FOSL1-PORCN-WNT4	7917	37593	48481	35640	51574	PITX2-PORCN-WNT2B	32916	28214	19614	42831	17840
FZD5-PORCN-WNT4	8507	37632	48747	30800	4942	FOSL1-PORCN-WNT2B	51756	54848	26032	20042	1751
KREMEN1-PORCN-WNT4	25014	55908	56360	6264	40529	FZD7-PORCN-WNT3A	601	7936	6391	14753	43442
DKK1-PORCN-WNT2B	13119	7914	33768	34345	53916	KREMEN1-PORCN-WNT3A	5432	49056	32287	41650	15766
BCL9-PORCN-WNT2B	31320	49751	15858	56923	5674	FZD8-PORCN-WNT4	16866	18194	19414	12569	12962
NLK-PORCN-WNT4	839	35865	37133	52537	3763	GSK3B-PORCN-WNT4	30196	41020	21974	56816	40470
FRAT1-PORCN-WNT4	1204	15349	9265	36000	46519	FZD6-PORCN-WNT2	2617	25245	12529	7270	8966
FZD5-PORCN-WNT2B	47626	21911	38180	411	51516	FZD6-PORCN-WNT5A	8901	16659	3797	41382	31216
CCND3-PORCN-WNT5A	39066	29570	4018	3443	56436	CXXC4-PORCN-WNT3	49304	25501	32130	16898	50343
FZD6-PORCN-WNT3A	41626	8812	22868	9411	30030	CSNK1D-PORCN-WNT5A	22402	4216	2288	18135	42734
BCL9-PORCN-WNT2	54955	22154	46038	51312	37377	DKK1-PORCN-WNT3A	34106	307	37594	26694	44252
EP300-PORCN-WNT4	22842	5697	24417	11816	30962	LRP5-PORCN-WNT5A	14554	31962	47440	55611	32184
FZD8-PORCN-WNT2	55228	25375	48312	22930	2643	CSNK1A1-PORCN-WNT4	39148	56389	5371	51550	11271
DIXDC1-PORCN-WNT2B	1674	21335	11428	19858	16898	CSNK1G1-PORCN-WNT2	44086	52040	53679	46699	15576
FOSL1-PORCN-WNT5A	51271	54488	32643	20512	3950	DAAM1-PORCN-WNT4	4715	18483	25056	27842	55467
FZD1-PORCN-WNT2	10972	56715	2891	54766	55230	EP300-PORCN-WNT2B	34780	53516	18975	9236	50588
DIXDC1-PORCN-WNT5A	16164	11219	7718	36336	22820	FOSL1-PORCN-WNT3A	49724	53367	21610	17015	8003
FZD2-PORCN-WNT3	16891	31724	13141	1509	53320	CSNK1A1-PORCN-WNT2B	51145	2966	1646	6984	51942
BCL9-PORCN-WNT3A	31080	25153	42987	49977	8016	FOSL1-PORCN-WNT2	6373	1865	49888	23145	13285
LEF1-PORCN-WNT3	53701	55441	52729	42382	1529	LRP6-PORCN-WNT2B	45427	12535	54497	51518	467
CTNNB1-PORCN-WNT2B	51347	1712	20034	6187	37020	FZD5-PORCN-WNT3A	44264	48407	37797	1058	40037
GSK3B-PORCN-WNT2B	10354	12749	19731	7003	20542	FZD2-PORCN-WNT4	34166	42118	26790	28126	260
FZD5-PORCN-WNT2	14336	48237	20369	3530	1362	EP300-PORCN-WNT5A	20231	51730	21290	6094	9403
FRAT1-PORCN-WNT5A	17074	33012	52	35018	11028	FRAT1-PORCN-WNT3A	56576	51355	16114	376	8592
KREMEN1-PORCN-WNT2	5726	54729	16213	7855	32505	CTNNBIP1-PORCN-WNT4	172	7513	38333	6376	48756
FZD7-PORCN-WNT2	5898	37770	3588	38329	46832	FBXW2-PORCN-WNT5A	21222	11676	43880	35992	48834
CSNK1A1-PORCN-WNT5A	54650	52431	7732	2602	47701	FRZB-PORCN-WNT5A	48028	29070	4466	31611	7573
FZD2-PORCN-WNT2	5093	52807	23045	18722	21837	FZD6-PORCN-WNT3	22555	18055	16279	1996	2337
DVL2-PORCN-WNT2B	34774	24150	6903	4977	15208	LEF1-PORCN-WNT4	5611	19412	56055	27914	1376
DIXDC1-PORCN-WNT2	9916	15221	5173	22635	55892	DVL1-PORCN-WNT2B	7994	25962	44952	31367	51921
FBXW11-PORCN-WNT2	4568	22339	17041	40983	5016	CTNNB1-PORCN-WNT5A	43762	3615	11416	6342	43345
DVL1-PORCN-WNT4	12806	51239	3810	47619	49456	FRAT1-PORCN-WNT3	23204	52743	26732	5703	32028
DAAM1-PORCN-WNT5A	35449	37756	36278	4984	18388	FBXW11-PORCN-WNT3	22335	39756	36822	12290	202
FBXW2-PORCN-WNT2	38497	36563	7161	13719	3870	DVL1-PORCN-WNT2	51914	20319	14179	47816	43578
DKK1-PORCN-WNT3	16889	6223	12205	44615	49416	FSHB-PORCN-WNT4	48407	41026	44326	38403	10738
DIXDC1-PORCN-WNT3A	50533	13326	45796	13169	18807	APC-PORCN-WNT3	31008	7341	12508	22839	3590
CSNK2A1-PORCN-WNT2	14811	7388	23266	45334	3849	DVL2-PORCN-WNT5A	25011	50148	30926	12099	23878
NLK-PORCN-WNT3	1151	51209	30649	40041	1150	GSK3B-PORCN-WNT3A	50592	9533	36087	5178	11848
FRZB-PORCN-WNT3A	43274	25499	6194	19063	9871	CTNNBIP1-PORCN-WNT5A	9002	40770	21026	25896	23350
CSNK1G1-PORCN-WNT3A	5132	49722	52426	55953	14853	FZD7-PORCN-WNT3	26004	2210	1421	15585	23223
FBXW2-PORCN-WNT3A	8868	7822	39246	38530	37536	CTNNBIP1-PORCN-WNT3	1806	45771	25025	3597	38354
FZD8-PORCN-WNT3	52647	14741	21742	5188	12616	DVL2-PORCN-WNT3A	56248	46719	21547	4335	32075
PORCN-SFRP1-WNT2B	11371	7274	38621	3196	33856	EP300-PORCN-WNT3	46942	10437	16688	1303	25139
PORCN-SFRP1-WNT5A	594	30254	46200	4810	32251	CSNK1A1-PORCN-WNT3	3737	47095	31808	23264	22340
LRP5-PORCN-WNT3	26284	10985	49664	49226	2910	FOSL1-PORCN-WNT3	8415	55	49545	34307	41439
AXIN1-PORCN-WNT4	3439	53381	53023	47853	2095	PORCN-WNT4-WNT5A	39548	22687	24609	57067	2189
FRAT1-PORCN-WNT2	16837	44503	5217	24876	44412	CTNNB1-PORCN-WNT3	18524	12386	36234	9685	30765
GSK3B-PORCN-WNT2	4811	27688	24895	50330	3255	AES-PORCN-WNT5A	47174	30282	25126	4019	12452
FRZB-PORCN-WNT3	2049	35897	28774	18126	55301	CTBP1-PORCN-WNT3A	19331	3013	43990	41658	27693
MYC-PORCN-WNT2	31464	54137	55028	11498	44754	DAAM1-PORCN-WNT2	1260	3063	21010	13636	38216
CTNNBIP1-PORCN-WNT2	6978	14005	25169	2753	40759	FGF4-PORCN-WNT2B	6331	344	43865	32471	20681

7.3.1. Examining the Behaviour of CTNNB1-PORCN-WNT3 Combination

Here we take up the case of CTNNB1-PORCN-WNT3 to examine its behaviour in time with respect to the recordings in Gujral and MacBeath [1] and the rankings of the combination across the four sensitivity methods.

Armadillo repeat is a repetitive amino acid sequence found in β-catenin. β-catenin is a protein that in humans is encoded by the CTNNB1 gene. β-Catenin was first discovered in McCrea et al. [31] as a component of a mammalian cell adhesion complex which is responsible for cytoplasmatic anchoring of cadherins. It acts as an intracellular signal transducer in the Wnt signaling pathway as shown by Peifer et al. [32] and Kemler [33]. It is known that the WNTs affect the downstream β-catenins. Also, PORCN help in the secretion of the WNTs and affects their activity. So a 3rd order axis is known to exist. Gujral and MacBeath [1] in their study recorded the activity of CTNNB1 also. Figure 1 shows the recordings of CTNNB1, PORCN and WNT3, each measured individually in Gujral and MacBeath [1]. Graphically, Figure 2 shows the changing rankings of CTNNB1-PORCN-WNT3 combination in time,

across different sensitivity analysis methods (i.e in Tables 2–5). Using the criteria used for considering a combination as showing conserved rankings, Figure 2 shows rankings in the range of 1 to 10,000, which lie above the threshold line (see figure). For HSIC linear, HSIC rbf and SOBOL martinez, it was found that the rankings were within the first 10,000 range, thus showing a majority out of four chosen sensitivity methods. Though passing a relaxed criteria across time, the machine learning search engine does point to the existence of the biological synergy between CTNNB1, PORCN and WNT3. Similar interpretations can be made for rankings of other combinations from the above tables.
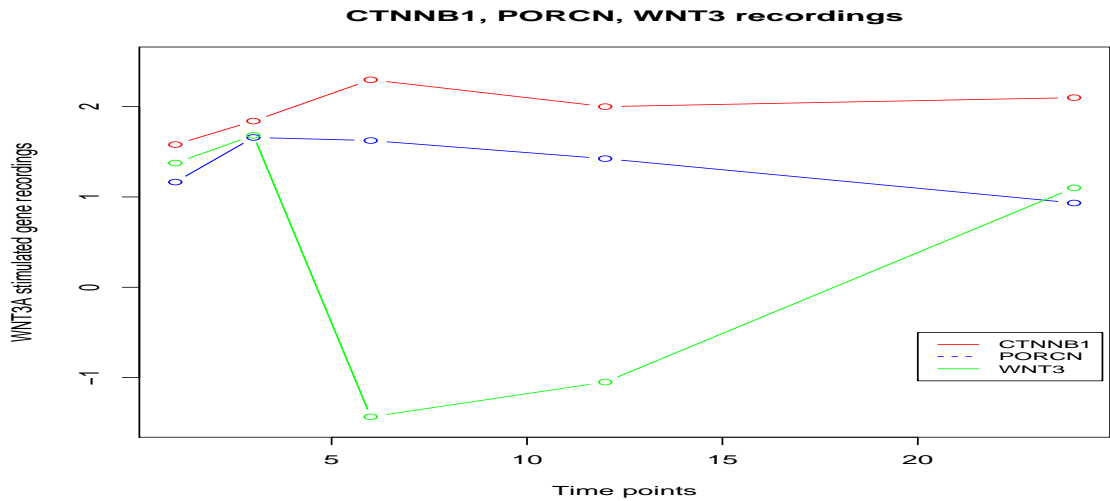

Figure 1. Recordings of CTNNB1, PORCN and WNT3, by Gujral and MacBeath [1] in WNT3A stimulated HEK 293 cells.
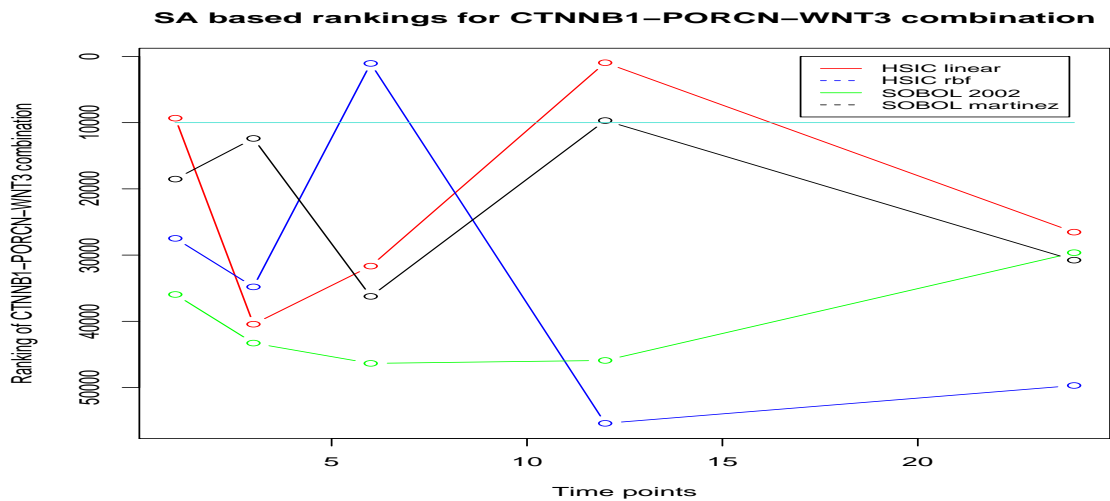

Figure 2. Rankings of 3rd order CTNNB1-PORCN-WNT3 combination, by the machine learning search engine, using different sensitivity methods.

7.4. Enumeration of top 10, 3rd Order Combinations for WNT3A Stimulated Response Genes

I now present the last section of the manuscript by tabulating 3rd order combinations of some of the WNT3A stimulated response genes, recorded by Gujral and MacBeath [1]. Out of the 71 response genes, I take a few genes with their family members for consideration. Further, I only present here combinations of interest, that were filtered using the machine learning search engine and those that passes the criteria for being termed conserved in rankings. Note that these combinations have either been established or require wet lab testing.

Table 6, shows the top 10 gene combinations involving a particular family of gene, that show conserved rankings across all four sensitivity methods. There are certain patterns that emerge from these rankings. I only cover these patters as experimental validations of them already exists. Nevertheless, on the basis of these experimentally established patterns, one can test remaining combinations that have yet to be explored and have been tabulated here.

Table 6. Top 10 3rd order combinations with conserved machine learning rankings of WNT3 stimulated response genes, across different sensitivity indices.

WNT3 stimulated response genes					
Response gene family	**Gene family member 3rd order combinations**				
adenomatosis polyposis coli (**APC**) regulator of WNT signaling pathway	APC-PITX2-SFRP4	APC-FZD6-SENP2	APC-PITX2-SENP2	APC-DIXDC1-WNT2B	APC-PITX2-TCF7	APC-FZD6-TLE2
	APC-FZD2-TCF7L1	APC-PITX2-PPP2CA	APC-PORCN-SENP2	APC-PITX2-WNT4		
v-myc avian myelocytomatosis viral oncogene homolog (**MYC**)	CSNK2A1-MYC-SENP2	CSNK2A1-MYC-SFRP4	AES-AXIN1-MYC	CSNK2A1-MYC-TCF7L1	FRZB-MYC-SENP2	CSNK2A1-MYC-PPP2CA
	DKK1-MYC-SENP2	FZD5-MYC-SENP2	CSNK2A1-MYC-WNT4	DVL1-MYC-SENP2		
frizzled class receptor (**FZD**)	FZD1	FZD2	FZD5	FZD6	FZD7	FZD8
	FZD1-NLK-SENP2	FSHB-FZD2-SENP2	FZD5-JUN-WNT2	APC-FZD6-FZD8	FZD7-NKD1-SENP2	FZD8-FBXW4-WNT3A
	AES-AXIN1-FZD1	FSHB-FZD2-WNT4	FZD5-JUN-FBXW4	APC-FZD6-TLE2	CXXC4-FZD7-PPP2CA	AES-AXIN1-FZD8
	DVL1-FRZB-FZD1	FSHB-FZD2-FZD7	FZD5-CCND2-FBXW11	AES-AXIN1-FZD6	FZD7-PPP2CA-SFRP4	FZD8-LRP6-RHOU
	FZD1-FZD7-PPP2CA	FSHB-FZD2-KREMEN1	FZD5-CCND2-SENP2	FZD6-PORCN-WNT2B	CXXC4-FZD7-SFRP4	FZD8-PORCN-SFRP1
	FZD1-FZD7-SFRP4	DKK1-FZD2-LRP5	FZD5-CCND2-FRZB	FZD6-PORCN-WNT4	FZD1-FZD7-PPP2CA	DIXDC1-FOXN1-FZD8
	AES-EP300-FZD1	APC-FZD2-TCF7L1	FZD5-CCND3-SENP2	FZD6-GSK3A-WNT2	FZD1-FZD7-SFRP4	FZD8-PORCN-SENP2
	DKK1-DVL2-FZD1	FSHB-FZD2-TLE2	FZD5-JUN-WNT5A	CCND1-CTBP1-FZD6	FZD7-PORCN-SENP2	CXXC4-FRAT1-FZD8
	CXXC4-FRAT1-FZD1	FSHB-FZD2-LRP5	FZD5-PITX2-SENP2	FZD6-PORCN-SENP2	CSNK1D-FGF4-FZD7	BTRC-FOXN1-FZD8
	DVL1-EP300-FZD1	FRZB-FZD2-SENP2	FZD5-CCND2-DKK1	FZD6-PORCN-TLE2	FSHB-FZD2-FZD7	FZD8-LRP6-TCF7
	FRAT1-FZD1-SFRP4	FSHB-FZD2-SFRP4	FZD5-MYC-SENP2	FZD6-PORCN-SFRP1	FZD7-PORCN-FBXW4	FZD8-GSK3A-KREMEN1
glycogen synthase kinase 3 (**GSK3**)	GSK3A			GSK3B		
	FRZB-GSK3A-SENP2			CSNK1D-FGF4-GSK3B		
	FRZB-GSK3A-PPP2R1A			FBXW11-GSK3B-WNT2B		
	DKK1-GSK3A-LRP5			FOSL1-FOXN1-GSK3B		
	FZD6-GSK3A-WNT2			GSK3B-LRP6-SLC9A3R1		
	BTRC-GSK3A-T			CTBP2-GSK3B-RHOU		
	FRZB-GSK3A-LRP5			CSNK1G1-GSK3B-SLC9A3R1		
	FZD5-GSK3A-SENP2			GSK3B-RHOU-SENP2		
	DKK1-GSK3A-WNT2B			FSHB-FZD2-GSK3B		
	BTRC-GSK3A-NLK			GSK3B-JUN-TLE1		
	CSNK1D-GSK3A-LEF1			CTBP1-FGF4-GSK3B		
dishevelled segment polarity protein (**DVL**)	DVL1			DVL2		
	DVL1-EP300-FRZB			DKK1-DVL2-SENP2		
	AXIN1-DVL1-FBXW2			DKK1-DVL2-FRZB		
	AXIN1-DVL1-FBXW11			DVL2-JUN-FBXW4		
	DVL1-FRZB-FZD1			DKK1-DVL2-FZD1		
	DVL1-EP300-GSK3B			DVL2-JUN-WNT3A		
	DVL1-EP300-WNT2B			DVL2-JUN-WNT2B		
	DVL1-FBXW11-SLC9A3R1			CXXC4-DVL2-FRZB		
	DVL1-EP300-WNT4			DKK1-DVL2-FBXW11		
	AXIN1-DVL1-RHOU			DVL2-JUN-TCF7		
	DVL1-EP300-FZD1			FZD5-DVL2-FRZB		
low density lipoprotein receptor related protein (**LRP**)	LRP5			LRP6		
	DVL1-EP300-LRP5			FBXW11-LRP6-SENP2		
	DKK1-JUN-LRP5			FBXW11-LRP6-TCF7		
	LRP5-NLK-WNT4			FBXW11-LRP6-SLC9A3R1		
	FOXN1-KREMEN1-LRP5			LRP6-TCF7-WNT2B		
	DKK1-FZD2-LRP5			FBXW11-LRP6-SFRP4		
	FZD5-FOXN1-LRP5			DKK1-LRP6-SENP2		
	FSHB-FZD2-LRP5			DAAM1-LRP6-SENP2		
	DKK1-GSK3A-LRP5			CCND2-LRP6-RHOU		
	LRP5-SFRP1-WNT2B			DAAM1-LRP6-SLC9A3R1		
	FRZB-GSK3A-LRP5			CCND2-LRP6-TCF7		
C-terminal binding protein (**CTBP**)	CTBP1			CTBP2		
	CCND1-CTBP1-KREMEN1			CTBP2-CTNNB1-FOSL1		
	CSNK2A1-CTBP1-PPP2R1A			CTBP2-CTNNB1-WNT4		
	CCND1-CTBP1-FZD6			CTBP2-T-TLE2		
	CTBP1-FGF4-FBXW4			CTBP2-FOXN1-SENP2		
	CTBP1-FGF4-FZD1			CTBP2-CTNNB1-FBXW4		
	CTBP1-FGF4-WNT5A			CTBP2-CTNNB1-TLE1		
	CTBP1-GSK3A-PPP2CA			CTBP2-CTNNB1-WNT2B		
	CTBP1-FGF4-TCF7L1			CTBP2-T-WNT2B		
	CTBP1-FGF4-FRZB			CTBP2-GSK3B-RHOU		
	CTBP1-FGF4-RHOU			CSNK1A1-CTBP2-KREMEN1		
cyclin D (**CCND**)	CCND1		CCND2		CCND3	
	CCND1-FGF4-GSK3B		CCND2-LRP6-SENP2		CCND3-PORCN-WNT4	
	CCND1-FGF4-RHOU		FZD5-CCND2-FBXW11		CCND3-PORCN-FBXW4	
	CCND1-WIF1-WNT2B		FZD5-CCND2-SENP2		FZD5-CCND3-SENP2	
	CCND1-FGF4-SFRP1		FZD5-CCND2-FRZB		FZD5-CCND3-FRZB	
	CCND1-FGF4-WNT5A		CCND2-LRP6-RHOU		AES-AXIN1-CCND3	
	CCND1-FGF4-FOSL1		CCND2-FBXW11-SLC9A3R1		CCND3-WNT1-WNT4	
	CCND1-PYGO1-WNT2		CCND2-LRP6-TCF7		CCND3-PORCN-SFRP1	
	CCND1-FGF4-FBXW4		FZD5-CCND2-DKK1		CCND3-PORCN-TLE2	
	CCND1-FGF4-PPP2R1A		CCND2-LRP6-FBXW4		FZD5-CCND3-CSNK1D	
	CCND1-CTBP1-KREMEN1		CCND2-WNT1-WNT4		FZD5-CCND3-SFRP4	
Wnt family member (**WNT**)	WNT1	WNT2B	WNT3A	WNT4	WNT5A	
	TLE2-WNT1-WNT2B	CTNNBIP1-WIF1-WNT2B	CSNK1D-FGF4-WNT3A	CXXC4-PORCN-WNT4	CSNK1D-FGF4-WNT5A	
	AXIN1-WNT1-WNT4	AES-AXIN1-WNT2B	FZD8-FBXW4-WNT3A	CSNK1D-FGF4-WNT4	FSHB-T-WNT5A	
	AXIN1-WNT1-WNT2	LRP6-TCF7-WNT2B	DKK1-JUN-WNT3A	LRP5-NLK-WNT4	CTNNBIP1-WIF1-WNT5A	
	CCND2-WNT1-WNT4	CXXC4-PORCN-WNT2B	AES-AXIN1-WNT3A	PITX2-PORCN-WNT4	CCND1-FGF4-WNT5A	
	TLE1-WNT1-WNT2B	TLE1-WIF1-WNT2B	DVL2-JUN-WNT3A	FSHB-FZD2-WNT4	FZD5-JUN-WNT5A	
	TCF7L1-WNT1-WNT2B	CCND1-WIF1-WNT2B	CCND1-FGF4-WNT3A	AXIN1-WNT1-WNT4	CCND2-LRP6-WNT5A	
	CCND2-WNT1-WNT5A	APC-DIXDC1-WNT2B	FBXW2-WNT3A-WNT4	DVL1-EP300-WNT4	PITX2-PORCN-WNT5A	
	TCF7L1-WNT1-WNT4	FZD7-NKD1-WNT2B	JUN-PYGO1-WNT3A	FSHB-T-WNT4	CXXC4-PORCN-WNT5A	
	TLE1-WNT1-WNT4	TLE2-WIF1-WNT2B	CTNNBIP1-WIF1-WNT3A	APC-PORCN-WNT4	LEF1-T-WNT5A	
	AXIN1-WNT1-WNT3		PPP2CA-WNT1-WNT3A	DKK1-JUN-WNT4	CXXC4-PORCN-WNT5A	

7.4.1. Adenomatosis Polyposis Coli (APC)

For APC, there are 5 combinations involving paired like homeodomain 2 (PITX2) with APC, thus depicting possible synergy between APC-PITX2 that need to explored. Kuraguchi et al. [34] showed that genetic deletion of APC in embryonic mouse oral epithelium (K14-Cre;APC$^{cko/cko}$) resulted in supernumerary tooth formation, thus suggesting that WNT signaling and the levels of APC are crucial determinants of tooth initiation. Following this, Wang et al. [35] observed that in APC$^{cko/cko}$ mice,

which express Cre recombinase uniformly throughout skin ectoderm and oral and dental epithelium, died at birth. Although their tooth germs appeared normal at E13.5, by E14.5 the mutant teeth were severely disrupted, with numerous irregular epithelial buds protruding from the oral epithelium into jaw mesenchyme, and intense expression of FGF8, SHH, PITX2, p21 and FGF4 transcripts and elevated levels of β-catenin. In Gujral and MacBeath [1], APC was found to be down regulated ($-ive$ numbers), while PITX2 was upregulated ($+ive$ numbers). The search engine confirms the existence of this biological synergy by pointing out 3rd order combinations involving APC-PITX2 interaction.

7.4.2. V-myc Avian Myelocytomatosis Viral Oncogene Homolog (MYC)

For MYC, there are 5 combinations involving casein kinase 2 α 1 (CSNK2A1) with MYC, and 5 combinations involving SUMO specific peptidase 2 (SENP2) with MYC. This depicts the possible synergy between MYC-CSNK2A1 and MYC-SENP2 that need to explored. Yang et al. [36] observed that CSNK2A1-mediated MAX phosphorylation increased C-MYC and β-catenin binding and regulated HMGB1 promoter activity through E-BOX. These further lead to promotion of cell growth, migration, and invasion and progression of cholangiocarcinogenesis. SENP1 is frequently overexpressed and correlates with the high expression of c-MYC, in breast cancer tissues. Sun et al. [37] found that SENP1, deSUMOylates c-MYC, resulting in its stabilization and activation. In Gujral and MacBeath [1], MYC was found to be up regulated ($+ive$ numbers) along with SENP2, and CSNK2A1 was found to show a transition from down regulation to up regulation and then down regulation. The search engine confirms the existence of this biological synergy by pointing out 3rd order combinations involving MYC-SENP2 and MYC-CSNK2A1 interaction.

7.4.3. fRizzled Class Receptor (FZD)

For FZD6, there are 5 combinations involving porcupine (PORCN) with FZD6. This depicts the possible synergy between FZD6-PORCN that need to explored. WNT ligands require palmitoylation by PORCN for their secretion and interaction with FZD receptors. Ghimire and Deans [38] in their analysis of PORCN CKOs suggest that the contribution of WNT signaling may be to establish the asymmetric distributions of FZD3, FZD6, and VANGL2 at the basolateral junctions between cochlear-supporting cells rather than as a diffusible attractant. In Gujral and MacBeath [1], FZD6 was found to be up regulated ($+ive$ numbers) along with PORCN. The search engine confirms the existence of this biological synergy by pointing out 3rd order combinations involving FZD6-PORCN interaction.

7.4.4. Glycogen Synthase Kinase 3 (GSK3)

For GSK3A (or α), there are 3 combinations involving frizzled related protein (FRZB) with GSK3A. This depicts the possible synergy between GSK3A-FRZB that need to explored. Jaka et al. [39] found that after silencing the FRZB gene, in the case of GSK3B (or β), lower level of phosphorylation was observed, and a lower P-GSK3B/GSK3B ratio, which suggested an increase in the activity of this kinase. Gujral and MacBeath [1], FRZB was found to be down regulated ($-ive$ numbers), while GSK3A was up regulated ($+ive$ numbers). The search engine confirms the existence of this biological synergy by pointing out 3rd order combinations involving FRZB-GSK3A interaction.

7.4.5. Dishevelled Segment Polarity Protein (DVL)

For DVL1, there are 5 combinations involving histone acetyltransferase E1A binding protein p300 (EP300) with DVL1. For DVL2, there are 4 combinations involving Jun proto-oncogene, AP-1 transcription factor subunit (JUN) with DVL2. This depicts the possible synergy between DVL1-EP300 and DVL2-JUN that need to explored. Zhong et al. [40] show that EP300 mutation and loss of GATA6 function bypassed the antidifferentiation activity of WNT signaling, rendering these cancer cells resistant to WNT inhibition. They point that consistent with the WNT-dependent nature of pancreatic cancer, many components of the WNT-signaling cascade were essential for cell growth. However, the extent of the dependencies was variable, which in some cases might be due to functional redundancy (e.g., DVL1 and DVL3). So there is a glimpse of possible synergy between DVL1 and EP300, that has

not been explored. Gan et al. [41] found that DVL and c-JUN form a complex with β-catenin–T-cell factor 4 (TCF-4) on the promoter of WNT target genes and regulate gene transcription. The complex forms via two interactions of nuclear DVL with c-JUN and β-catenin, respectively, both of which bind to TCF. Here, the interaction between DVL and JUN is already established. Gujral and MacBeath [1], DVL-1/2 was found to be up regulated (+*ive* numbers), while EP300 and JUN were also up regulated (+*ive* numbers). The search engine confirms the existence of the biological synergy between the above components by pointing out 3rd order combinations involving DVL1-EP300 and DVL2-JUN interaction.

7.4.6. Low Density Lipoprotein Receptor-Related Protein (LRP)

For LRP6, there are 4 combinations involving F-box and WD repeat domain containing 11 (FBXW11) with LRP6. This depicts the possible synergy between LRP6-FBXW11 that need to be explored. Wang et al. [42] state that upon activation of the pathway by the binding of Wnt ligand to Frizzled and LRP5–LRP6 receptors, the axin complex is inhibited and results in the accumulation of soluble β-catenin that can enter the nucleus, where it interacts with transcription factors of the TCF/LEF1 family to regulate a series of target genes. It is assumed that APC helps phosphorylated β-catenin to dissociate from AXIN, creating a catalytic cycle of binding and release of the substrate. Others have suggested that APC acts either upstream of the phosphorylation reactions, by transporting β-catenin to the complex or downstream of the phosphorylation reactions, by recruiting the ubiquitin ligase bTrCP (FBXW11) to the complex. Holt et al. [43] observe that FBXW11 targets include β-catenin, key mediator of WNT signaling, critical to digital, neurological, and eye development. There might be an indirect synergy between LRP6-FBXW11. Gujral and MacBeath [1], LRP6 was found to be up regulated (+*ive* numbers), along with FBXW11. The search engine confirms the possible existence of the biological synergy between the above components by pointing out 3rd order combinations involving LRP6-FBXW11 interaction.

7.4.7. C-Terminal Binding Protein (CTBP)

For CTBP1, there are 6 combinations involving fibroblast growth factor 4 (FGF4) with CTBP1. For CTBP2, there are 5 combinations involving catenin β 1 (CTNNB1) with CTBP2. This depicts the possible synergy between CTBP1-FGF4 and CTBP2-CTNNB1 that need to explored. Wang et al. [42] observe that during the epithelial–mesenchymal transition (EMT) process, TGFβ induced isoform switching of FGF receptors, causing the cells to become sensitive to FGF2. Addition of FGF2 to TGFβ-treated cells perturbed EMyoT by reactivating the MEK-Erk pathway and subsequently enhanced EMT through the formation of MEK-Erk-dependent complexes of the transcription factor δEF1/ZEB1 with the transcriptional corepressor CTBP1. Kim et al. [44] demonstrate that CTBP2 associates with major components of the β-catenin (CTNNB1) destruction complex and limits the accessibility of β-catenin to core transcription factors in undifferentiated embryonic stem cells (ESCs). Thus the synergies between the components have been established. Gujral and MacBeath [1], CTBP-1/2 and CTNNB1 were found to be up regulated (+*ive* numbers), while FGF4 was down regulated for a major period of time (apart from being upregulated). The search engine confirms the possible existence of the biological synergy between the above components by pointing out 3rd order combinations involving CTBP1-FGF4 and CTBP2-CTNNB1 interactions.

7.4.8. Cyclin D (CCND)

For CCND1, there are 7 combinations involving fibroblast growth factor 4 (FGF4) with CCND1. For CCND-2/3, there are 4 combinations each involving frizzled class receptor 5 (FZD5) with CCND-1/2. This depicts the possible synergy between CCND1-FGF4 and CCND-1/2-FZD5 that need to explored. Bao et al. [45] show that CCND1 co-localizes with FGF3, FGF4, and FGF19 at chromosome location 11q13. Brandt et al. [46] show that expression levels of previously described endothelial target genes of β-catenin were studied using qPCR, but no differences was observed in the expression of CCND1 after knockdown of FZD5. But this might not be the case with CCND-2/3. Gujral and

MacBeath [1], CCND-1/2/3 was found to be up regulated ($+ive$ numbers) along with FGF4, while FZD5 was found to be down regulated ($-ive$ numbers). The search engine confirms the possible existence of the biological synergy between the above components by pointing out 3rd order combinations involving CCND1-FGF4 and CCND-2/3-FZD5 interactions.

7.4.9. Wnt Family Member (WNT)

One peculiarity that we can find in the table under the title of WNT1 is that the machine points to synergistic combinations of WNT1 with other families of WNT. This pattern emerged in all the top 10 ranked combinations. It might be of interest to investigate whether WNT1 works in tandem with other WNT family members, as if one observes in the other columns such behaviour is not observed.

8. Conclusion

This study demonstrates how biologists can use the machine learning based search engine to address the needle in a haystack problem of discovering meaningful combinations of higher order in a vast search forest, which on further wet lab test might assist in intervening the pathway at a combinatorial level, in time. The problem explodes combinatorially with even a small set of recorded genes in the above study, when one steps to explore 3rd order combinations. With the total number of C_3^{71} (= 57155) combinations in this study, it becomes nearly impossible for any biologist to study the system wide dynamics of any pathway. The manuscript addresses these issues by enumerating and ranking a huge list of 3rd order combinations, demonstrating conserved machine learning rankings for wet lab established combinations across the different sensitivity methods used and presenting some of the patterns in the behaviour of some of the established combinations related to WNT3A response genes. In summary, the work presents a solution to the fundamental needle in a haystack problem of locating higher order gene combinations in a vast search forest, via use of powerful machine learning based search engine. Use of this engine is bound to assist many biologists/oncologists in search for meaningful higher order gene combinations that work in cell biology and make potential discoveries necessary for advancement in the study of cell/developmental biology as well as developement of therapeutics in diseased cells.

Competing interests

No competing interest is declared.

Author contributions statement

SS conceived and designed the experiments; wrote the code; performed the experiments; analyzed the data; wrote the manuscript.

Availability of code

Code for time series data available at CERN based Zenodo on https://zenodo.org/records/14637456.

Acknowledgments

Special thanks to Mrs. Rita Sinha and late Mr. Prabhat Sinha for supporting the author financially, without which this work could not have been made possible.

Supplementary

The following files (ending with .R and can be opened in R or in simple text processing program) with these names are made available with this manuscript. (1) **HSIClinear-TP-Choose-3-NSc-D.R**, (2) **HSICrbf-TP-Choose-3-NSc-D.R**, (3) **SB2002-TP-Choose-3-NSc-D.R**, and (4) **SBmartinez-TP-Choose-3-NSc-D.R**, contain rankings for 3rd order combinations across each time point for, HSIC (linear

kernel), HSIC (rbf kernel), SOBOL (2002 implementation) and SOBOL (martinez implementation), respectively.

References

1. Gujral, T.S.; MacBeath, G. A system-wide investigation of the dynamics of Wnt signaling reveals novel phases of transcriptional regulation. *PloS one* **2010**, *5*, e10024.
2. Sinha, S. Machine learning ranking of plausible (un) explored synergistic gene combinations using sensitivity indices of time series measurements of Wnt signaling pathway. *Integrative Biology* **2024**, *16*, zyae020.
3. Joachims, T. Training linear SVMs in linear time. In Proceedings of the Proceedings of the 12th ACM SIGKDD international conference on Knowledge discovery and data mining. ACM, 2006, pp. 217–226.
4. Sharma, R. Wingless a new mutant in Drosophila melanogaster. *Drosophila information service* **1973**, *50*, 134–134.
5. Thorstensen, L.; Lind, G.E.; Løvig, T.; Diep, C.B.; Meling, G.I.; Rognum, T.O.; Lothe, R.A. Genetic and epigenetic changes of components affecting the WNT pathway in colorectal carcinomas stratified by microsatellite instability. *Neoplasia* **2005**, *7*, 99–108.
6. Baron, R.; Kneissel, M. WNT signaling in bone homeostasis and disease: from human mutations to treatments. *Nature medicine* **2013**, *19*, 179–192.
7. Clevers, H. Wnt/[β]-catenin signaling in development and disease. *Cell* **2006**, *127*, 469–480.
8. Sokol, S. *Wnt Signaling in Embryonic Development*; Vol. 17, Elsevier, 2011.
9. Pinto, D.; Gregorieff, A.; Begthel, H.; Clevers, H. Canonical Wnt signals are essential for homeostasis of the intestinal epithelium. *Genes & development* **2003**, *17*, 1709–1713.
10. Zhong, Z.; Ethen, N.J.; Williams, B.O. WNT signaling in bone development and homeostasis. *Wiley Interdisciplinary Reviews: Developmental Biology* **2014**, *3*, 489–500.
11. Pećina-Šlaus, N. Wnt signal transduction pathway and apoptosis: a review. *Cancer Cell International* **2010**, *10*, 1–5.
12. Kahn, M. Can we safely target the WNT pathway? *Nature Reviews Drug Discovery* **2014**, *13*, 513–532.
13. Garber, K. Drugging the Wnt pathway: problems and progress. *Journal of the National Cancer Institute* **2009**, *101*, 548–550.
14. Voronkov, A.; Krauss, S. Wnt/beta-catenin signaling and small molecule inhibitors. *Current pharmaceutical design* **2012**, *19*, 634.
15. Blagodatski, A.; Poteryaev, D.; Katanaev, V. Targeting the Wnt pathways for therapies. *Mol Cell Ther* **2014**, *2*, 28.
16. Curtin, J.C.; Lorenzi, M.V. Drug discovery approaches to target Wnt signaling in cancer stem cells. *Oncotarget* **2010**, *1*, 552.
17. Bänziger, C.; Soldini, D.; Schütt, C.; Zipperlen, P.; Hausmann, G.; Basler, K. Wntless, a conserved membrane protein dedicated to the secretion of Wnt proteins from signaling cells. *Cell* **2006**, *125*, 509–522.
18. Bartscherer, K.; Pelte, N.; Ingelfinger, D.; Boutros, M. Secretion of Wnt ligands requires Evi, a conserved transmembrane protein. *Cell* **2006**, *125*, 523–533.
19. Kurayoshi, M.; Yamamoto, H.; Izumi, S.; Kikuchi, A. Post-translational palmitoylation and glycosylation of Wnt-5a are necessary for its signalling. *Biochemical Journal* **2007**, *402*, 515–523.
20. Gao, X.; Hannoush, R.N. Single-cell imaging of Wnt palmitoylation by the acyltransferase porcupine. *Nature chemical biology* **2014**, *10*, 61–68.
21. Sinha, S. Hilbert-Schmidt and Sobol sensitivity indices for static and time series Wnt signaling measurements in colorectal cancer-part A. *BMC systems biology* **2017**, *11*, 120.
22. Da Veiga, S. Global sensitivity analysis with dependence measures. *Journal of Statistical Computation and Simulation* **2015**, *85*, 1283–1305.
23. Saltelli, A. Making best use of model evaluations to compute sensitivity indices. *Computer physics communications* **2002**, *145*, 280–297.
24. Martinez, J. Analyse de sensibilite globale par decomposition de la variance. *Presentation in "Journée des GdR Ondes & Mascot* **2011**, *13*, 207.
25. Baudin, M.; Boumhaout, K.; Delage, T.; Iooss, B.; Martinez, J.M. Numerical stability of Sobol'indices estimation formula. In Proceedings of the Proceedings of the 8th International Conference on Sensitivity Analysis of Model Output (SAMO 2016), 2016, Vol. 30, pp. 50–51.

26. Tanaka, K.; Okabayashi, K.; Asashima, M.; Perrimon, N.; Kadowaki, T. The evolutionarily conserved porcupine gene family is involved in the processing of the Wnt family. *European Journal of Biochemistry* **2000**, *267*, 4300–4311.

27. Liu, J.; Xiao, Q.; Xiao, J.; Niu, C.; Li, Y.; Zhang, X.; Zhou, Z.; Shu, G.; Yin, G. Wnt/β-catenin signalling: function, biological mechanisms, and therapeutic opportunities. *Signal transduction and targeted therapy* **2022**, *7*, 3.

28. Willert, K.; Brown, J.D.; Danenberg, E.; Duncan, A.W.; Weissman, I.L.; Reya, T.; Yates III, J.R.; Nusse, R. Wnt proteins are lipid-modified and can act as stem cell growth factors. *Nature* **2003**, *423*, 448–452.

29. Liu, J.; Pan, S.; Hsieh, M.H.; Ng, N.; Sun, F.; Wang, T.; Kasibhatla, S.; Schuller, A.G.; Li, A.G.; Cheng, D.; et al. Targeting Wnt-driven cancer through the inhibition of Porcupine by LGK974. *Proceedings of the National Academy of Sciences* **2013**, *110*, 20224–20229.

30. Madan, B.; Ke, Z.; Harmston, N.; Ho, S.Y.; Frois, A.; Alam, J.; Jeyaraj, D.A.; Pendharkar, V.; Ghosh, K.; Virshup, I.H.; et al. Wnt addiction of genetically defined cancers reversed by PORCN inhibition. *Oncogene* **2016**, *35*, 2197–2207.

31. McCrea, P.D.; Turck, C.W.; Gumbiner, B. A homolog of the armadillo protein in Drosophila (plakoglobin) associated with E-cadherin. *Science* **1991**, *254*, 1359–1361.

32. Peifer, M.; Rauskolb, C.; Williams, M.; Riggleman, B.; Wieschaus, E. The segment polarity gene armadillo interacts with the wingless signaling pathway in both embryonic and adult pattern formation. *Development* **1991**, *111*, 1029–1043.

33. Kemler, R. From cadherins to catenins: cytoplasmic protein interactions and regulation of cell adhesion. *Trends in Genetics* **1993**, *9*, 317–321.

34. Kuraguchi, M.; Wang, X.P.; Bronson, R.T.; Rothenberg, R.; Ohene-Baah, N.Y.; Lund, J.J.; Kucherlapati, M.; Maas, R.L.; Kucherlapati, R. Adenomatous polyposis coli (APC) is required for normal development of skin and thymus. *PLoS genetics* **2006**, *2*, e146.

35. Wang, X.P.; O'Connell, D.J.; Lund, J.J.; Saadi, I.; Kuraguchi, M.; Turbe-Doan, A.; Cavallesco, R.; Kim, H.; Park, P.J.; Harada, H.; et al. Apc inhibition of Wnt signaling regulates supernumerary tooth formation during embryogenesis and throughout adulthood **2009**.

36. Yang, B.; Zhang, J.; Wang, J.; Fan, W.; Barbier-Torres, L.; Yang, X.; Justo, M.A.R.; Liu, T.; Chen, Y.; Steggerda, J.; et al. CSNK2A1-mediated MAX phosphorylation upregulates HMGB1 and IL-6 expression in cholangiocarcinoma progression. *Hepatology Communications* **2023**, *7*, e00144.

37. Sun, X.X.; Chen, Y.; Su, Y.; Wang, X.; Chauhan, K.M.; Liang, J.; Daniel, C.J.; Sears, R.C.; Dai, M.S. SUMO protease SENP1 deSUMOylates and stabilizes c-Myc. *Proceedings of the National Academy of Sciences* **2018**, *115*, 10983–10988.

38. Ghimire, S.R.; Deans, M.R. Frizzled3 and Frizzled6 cooperate with Vangl2 to direct cochlear innervation by type II spiral ganglion neurons. *Journal of Neuroscience* **2019**, *39*, 8013–8023.

39. Jaka, O.; Casas-Fraile, L.; Azpitarte, M.; Aiastui, A.; De Munain, A.L.; Saenz, A. FRZB and melusin, overexpressed in LGMD2A, regulate integrin β1D isoform replacement altering myoblast fusion and the integrin-signalling pathway. *Expert Reviews in Molecular Medicine* **2017**, *19*, e2.

40. Zhong, Z.; Harmston, N.; Wood, K.C.; Madan, B.; Virshup, D.M.; et al. A p300/GATA6 axis determines differentiation and Wnt dependency in pancreatic cancer models. *The Journal of Clinical Investigation* **2022**, *132*.

41. Gan, X.q.; Wang, J.y.; Xi, Y.; Wu, Z.l.; Li, Y.p.; Li, L. Nuclear Dvl, c-Jun, β-catenin, and TCF form a complex leading to stabiLization of β-catenin–TCF interaction. *The Journal of cell biology* **2008**, *180*, 1087–1100.

42. Wang, L.; Liu, X.; Gusev, E.; Wang, C.; Fagotto, F. Regulation of the phosphorylation and nuclear import and export of β-catenin by APC and its cancer-related truncated form. *Journal of cell science* **2014**, *127*, 1647–1659.

43. Holt, R.J.; Young, R.M.; Crespo, B.; Ceroni, F.; Curry, C.J.; Bellacchio, E.; Bax, D.A.; Ciolfi, A.; Simon, M.; Fagerberg, C.R.; et al. De novo missense variants in FBXW11 cause diverse developmental phenotypes including brain, eye, and digit anomalies. *The American Journal of Human Genetics* **2019**, *105*, 640–657.

44. Kim, T.W.; Kwak, S.; Shin, J.; Kang, B.H.; Lee, S.E.; Suh, M.Y.; Kim, J.H.; Hwang, I.Y.; Lee, J.H.; Choi, J.; et al. Ctbp2-mediated β-catenin regulation is required for exit from pluripotency. *Experimental & molecular medicine* **2017**, *49*, e385–e385.

45. Bao, Y.; Gabrielpillai, J.; Dietrich, J.; Zarbl, R.; Strieth, S.; Schröck, F.; Dietrich, D. Fibroblast growth factor (FGF), FGF receptor (FGFR), and cyclin D1 (CCND1) DNA methylation in head and neck squamous cell carcinomas is associated with transcriptional activity, gene amplification, human papillomavirus (HPV) status, and sensitivity to tyrosine kinase inhibitors. *Clinical Epigenetics* **2021**, *13*, 1–18.

46. Brandt, M.M.; Van Dijk, C.G.; Chrifi, I.; Kool, H.M.; Bürgisser, P.E.; Louzao-Martinez, L.; Pei, J.; Rottier, R.J.; Verhaar, M.C.; Duncker, D.J.; et al. Endothelial loss of Fzd5 stimulates PKC/Ets1-mediated transcription of Angpt2 and Flt1. *Angiogenesis* **2018**, *21*, 805–821.